On Savitzky-Golay Filtering for Online Condition Monitoring of Transformer On-Load Tap Changer

Article *in* IEEE Transactions on Power Delivery · September 2017

DOI: 10.1109/TPWRD.2017.2749374

3 authors:

Junhyuck Seo
The University of Queensland

Hui Ma
The University of Queensland

Tapan Kumar Saha
The University of Queensland

On Savitzky-Golay Filtering for Online Condition Monitoring of Transformer On-Load Tap Changer

Junhyuck Seo *Student Member, IEEE*, Hui Ma, *Senior Member, IEEE*, and Tapan Saha, *Senior Member, IEEE*
School of Information Technology and Electrical Engineering
University of Queensland
Brisbane, QLD 4072, Australia

***Abstract*— Vibro-acoustic measurement on a transformer's On-Load Tap Changer (OLTC) can provide indications on its mechanical condition. Recently, a joint vibro-acoustic and arcing measurement system has been proposed, which can correlate the vibro-acoustic signal to mechanical events of OLTC's operation. However, there are still considerable difficulties in extracting useful information from both vibro-acoustic signal and arcing signal in a synchronized manner without any distortions in the extracted signals. In this paper, Savitzky-Golay filter is introduced to process the signals acquired from a joint vibro-acoustic and arcing measurement system installed on in-service OLTCs. It proves that the Savitzky-Golay filter can process both vibro-acoustic and arcing signals induced by OLTC, extract essential information without any time delay from both types of signals, and retrieve voltage phase information from the arcing signal. The methodologies developed in this paper can improve the visibility of OLTC's mechanical operation for an effective online condition monitoring.**

Keywords*— arcing; condition monitoring; On-load Tap Changer (OLTC); phase information; power transformer; Savitzky-Golay filter; vibro-acoustic.

I. Introduction

Among various techniques for On-Load Tap Changer (OLTC) condition monitoring, vibro-acoustic measurement can be performed online without disturbing OLTC and transformer operation [1-5]. Vibro-acoustic measurement is useful in detecting change in mechanical condition at different stages of an OLTC's service life. Any such changes can be reflected by identifying the transition of the magnitude and time-of-occurrence of the measured vibro-acoustic signal acquired during OLTC's operation [1-5].

However, considerable difficulties still exist in identifying the time stamps (time-of-occurrences) of the measured vibro-acoustic signals and correlating these time stamps to the corresponding events of an OLTC's mechanical operations [5]. Such challenges may impair the effectiveness of the vibro-acoustic measurement or the recently proposed joint vibro-acoustic and arcing measurement for OLTC condition monitoring [6].

A number of signal processing techniques have been applied for analyzing OLTC's vibro-acoustic signals [1-2, 4-5]. Several researchers adopted wavelet transform [1, 4]. Instead of directly dealing with the original measured signal and explicitly finding the signals peaks and widths with time stamps, they attempted to smooth vibro-acoustic signals' waveforms using wavelet approximation. The smoothed (simplified) waveforms were then used to investigate any condition change in the OLTC. However, in the above wavelet approximation approaches, selecting a suitable mother wavelet and deciding appropriate decomposition levels are not trivial tasks for obtaining a satisfactory approximation. Low pass filter (LPF) has also been used to simplify vibro-acoustic signals [7].

A major drawback of using wavelet approximation or the low pass filter is that it causes time shifts between the original and filtered signals. Such time disparity can cause difficulties in matching and aligning among signals for analysis. Furthermore, the parameters of wavelet approximation and low pass filter can be affected by many factors such as the construction of OLTC, the characteristics of sensors and measurement system, and environmental conditions.

To complement the lack of interpretability of vibro-acoustic signal on OLTC's operation, a joint vibro-acoustic and arcing measurement method has been proposed [6]. In this method, a high frequency current transducer (HFCT) was clamped on the transformer's grounding cable to measure arcing signal in parallel with acoustic sensors used to measure the vibro-acoustic signal. The arcing signal corresponds to the event of OLTC switching contact closing at a tap position. By combining both signals, information of OLTC's mechanical events can be derived to facilitate an improved OLTC condition monitoring. The time alignment of signals is important in the joint vibro-acoustic and arcing measurement since the time discrepancy between the signals can cause a misinterpretation on the condition of switching contacts and the source of mechanical event. However, it is challenging to process vibro-acoustic and arcing signals simultaneously, especially preserving the event time information of two different types of signals from time discrepancies.

This paper proposes to apply Savitzky-Golay filter to process both vibro-acoustic and arcing signals to act as a joint measurement system for OLTC condition monitoring. The benefit of using Savitzky-Golay filter is that, regardless of the severity of filtering, it can extract the required profiles and information from the signal without causing any time gap. This is because it computes each individual data point by acquiring a local least-squared polynomial approximation of the signal. After a thorough investigation into the filter parameters, optimal Savitzky-Golay filters specific to the application have been designed in the paper. These filters are then used to process vibro-acoustic and arcing signals acquired from the joint measurement system installed on two types of in-service OLTCs. It will be demonstrated that Savitzky-Golay filter can acquire the profile of the vibro-acoustic signal and extract arcing signal from noise without any time change, as well as identify AC phase information from the measured arcing signal. The result can be used to support the interpretation of OLTC's operational sequence in online condition monitoring.

This paper is organized as follows. The joint vibro-acoustic and arcing signal measurement method is briefly reviewed in Section II. The mathematical formulation of Savitzky-Golay filter is discussed in Section III. Section IV and VI details three major applications of the Savitzky-Golay filter to analyze vibro-acoustic signal and arcing signal respectively. Section VII verifies the applicability of the proposed Savitzky-Golay filter through field measurement case studies on two different types of in-service OLTCs. Lastly, Section VIII concludes this paper.

II. Joint Vibro-Acoustic and Arcing Measurement System for OLTC's Condition Monitoring

During an OLTC operation, a series of events are generated at different time instances. These events induce acoustic waves, which can be measured by vibro-acoustic sensors attached on the outside wall of a transformer. When an OLTC's switching contact closes at a tap position arcing occurs, and its corresponding electromagnetic signals flow to the transformer's grounding cable and secondary phase connection cables. By clamping a HFCT on the grounding cable or the phase connection cables, the arcing signal can be captured. Together with the current signal of OLTC's motor drive system, the above combination of vibro-acoustic signal and arcing signal measurements can provide a better interpretation and visibility of OLTC's operation, especially the close/open events of its switching contacts. Such interpretation can improve the condition monitoring of OLTC.

Fig. 1 depicts the schematic of the joint vibro-acoustic and arcing signal measurement system. An acoustic emission sensor (frequency range is 50 – 400 kHz) and several HFCTs (frequency range is 350 kHz – 35 MHz) were employed. A current transformer (CT) is also used to measure OLTC's motor current. All sensor measurements are fed into a data acquisition system. The sampling rate was set to one Mega Samples/Second. To capture four consecutive OLTC operations (up/down/down/up), signals were recorded for 50 seconds. Fig. 2 presents an example of measured vibro-acoustic signal and arcing signal.

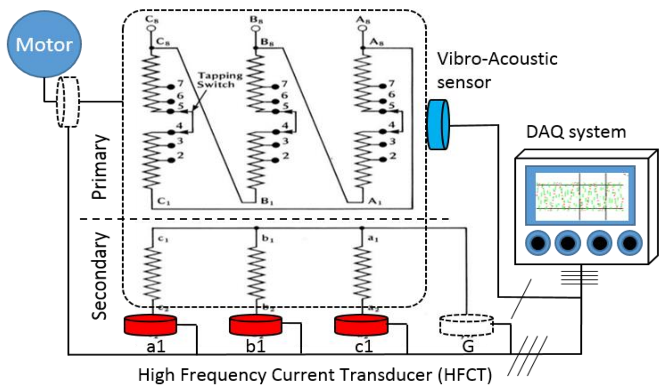

Fig. 1. A joint vibro-acoustic and arcing measurement system for OLTC condition monitoring (HFCTs at a1, b1, and c1 are clamped on three phase connection cables, a HFCT at G is clamped on the transformer grounding cable).

As shown in Fig. 2, signal processing needs to be performed on the measured vibro-acoustic and arcing signals for inferring the mechanical events involved in OLTC operation. In [7], a LPF was applied to smooth the vibro-acoustic signal while a probabilistic wavelet transform algorithm was applied to extract arcing signal from noise and harmonics. However, such arrangements may still have two issues: (1) time delay can exist between the originally measured signal and the smoothed/extracted signal, which leads to misalignment between the vibro-acoustic signal and the arcing signal; and (2) the probabilistic wavelet transform algorithm can be time-consuming in extracting arcing signal.

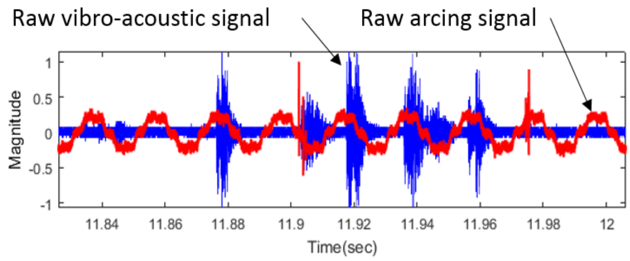

Fig. 2. Vibro-acoustic and arcing signals of an in-service OLTC at field.

This paper addresses the above two issues by applying the Savitzky-Golay filter to capture the profile of vibro-acoustic signal and extract arcing signal from noise and harmonics. The Savitzky-Golay filter does not cause any time gap in processing and thus maintains the synchronization between these two signals.

III. A Review on Savitzky-Golay Filter

The Savitzky-Golay filter uses the local least-squared polynomial approximation to smooth a signal to generate an envelope curve (profile) of the signal. It has the advantages of preserving the peaks and widths of the original signal while discarding its noise components at different frequencies. Such properties would be attractive for processing OLTC vibro-acoustic signal [8-10]. Fig. 3 illustrates the idea behind Savitzky-Golay filter.

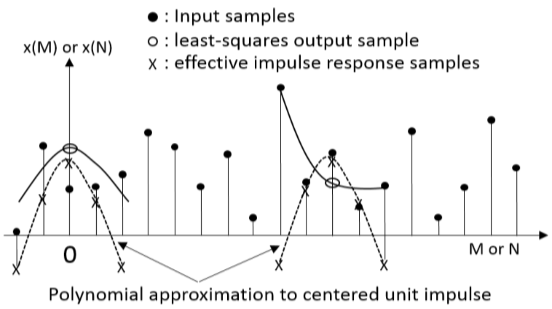

Fig. 3. Illustration of the Savitzky-Golay filter.

Let $x[n]$ denote a series of samples of a signal. By selecting $2M+1$ samples centered at $n = 0$, one can find a series of coefficients of a polynomial [9]

$$p(n) = \sum_{k=0}^{N} a_k n^k \quad (1)$$

which minimizes a mean-squared error ϵ_N as

$$\sum_{n=-M}^{M}(p(n) - x[n])^2 = \sum_{n=-M}^{M}\left(\sum_{k=0}^{N} a_k n^k - x[n]\right)^2 \quad (2)$$

As an example, in Fig. 3 (left hand side of the graph), $p(n)$ is evaluated at an approximation interval of $[-2, 2]$ and the smoothed output is obtained at the center of this interval. The output $y[0] = p(0) = a_0$ equals to the 0-*th* polynomial coefficient. In practice the approximation interval may not necessarily be symmetric with respect to the evaluation point. The whole process of the Savitzky-Golay filtering is:

1) Right shifting the interval by one sample.
2) Making the position of the middle sample of total $2M + 1$ samples as the new origin.
3) Performing the polynomial fitting and evaluation at the new origin. This process is repeated until the last sample in $2M + 1$ samples.

To find the optimal coefficients for the polynomial in (1), differentiate ϵ_N for $i = 0, 1, \ldots, N$ (total $N + 1$ unknown coefficients) and then set the corresponding derivative to zero as

$$\frac{\partial \epsilon_N}{\partial a_i} = \sum_{n=-M}^{M} 2n^i \left(\sum_{k=0}^{N} a_k n^k - x[n]\right) = 0 \quad (3)$$

By interchanging the order of the summations, a set of $N + 1$ equations with $N + 1$ unknowns can be formulated [9]

$$\sum_{n=0}^{N}\left(\sum_{n=-M}^{M} n^{i+k}\right) a_k = \sum_{n=-M}^{M} n^i x[n]\,, i = 0, 1, \ldots, N \quad (4)$$

The equations in (4) are the normal equations for the least-squared approximation problem. It is worth mentioning that solving (4) requires $2M \geq N$ samples. If the order of the polynomial (N) is too large, there would be no solutions for (4) since the approximation problem for this case will be poorly conditioned.

A properly designed Savitzky-Golay filter can preserve the waveform of an oversampled but noise-corrupted signal. Such performance of the Savitzky-Golay filter is more obvious in the frequency domain; the filter's output is extremely flat in the pass-band with modest attenuation in the stop-band [9]. Since the symmetric Savitzky-Golay filter has zero phase, it does not introduce any feature shift with respect to the original signal.

IV. Savitzky-Golay Filter to Analyze Vibro-Acoustic Signal of OLTC

This section presents the extraction of envelope curve from OLTC vibro-acoustic signal using Savitzky-Golay filter with properly selected parameters (frame size and order of polynomial). It also provides a performance comparison among Savitzky-Golay filter, low pass filter (LPF), and wavelet's approximation in processing OLTC's vibro-acoustic signal.

A. Pre-processing Vibro-Acoustic Signal

As shown in Fig. 2, the measured OLTC's vibro-acoustic signal exhibits a fast commutation between positive and negative polarities. Before performing Savitzky-Golay filtering, it is important to determine an appropriate vibro-acoustic signal representation for the filter input. Three possible representation to the filter are:

1. The spline curve using peaks in positive polarity.
2. The spline curve using peaks in both positive and negative polarities (negative polarity is reverted in the spline curve).
3. The absolute value of the original signal.

Fig. 4 presents the above first two spline curves. It can be seen that the spline curve using peaks only in positive polarity (black dotted line) is smoother than the spline curve using peaks in both positive and negative polarities (red dotted line). The third type of input for the filter takes the absolute value of the measured vibro-acoustic signal instead of using any spline curve of the signal.

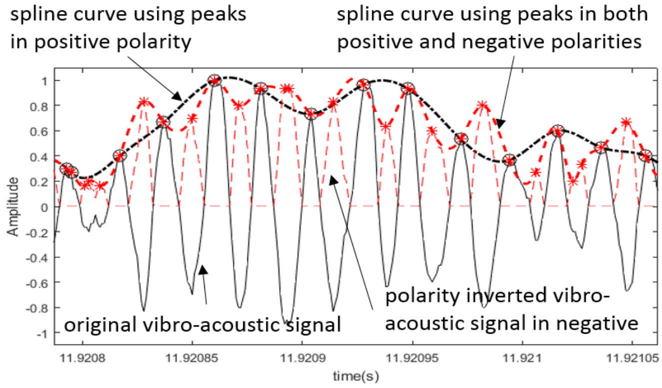

Fig. 4. (1) Spline curve using peaks in positive polarity (black dotted line); and (2) Spline curve using peaks in both positive and negative polarities (red dotted line).

Using the above three inputs, three Savitzky-Golay filters were implemented with the same parameters of frame size and order of polynomial. Fig. 5 presents the results of these Savitzky-Golay filters. It can be seen that the Savitzky-Golay filter using the spline curve with peaks in both positive and negative polarities (red dotted line in Fig. 5) generated more fluctuated waveform compared to the other two filters. This is because the signal's peaks in the positive and negative polarities are not strictly symmetric with respect to the X axis as seen in Fig. 4.

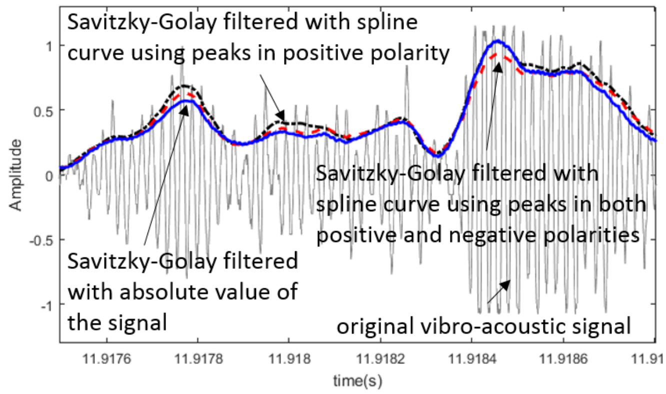

Fig. 5. Results of Savitzky-Golay filters with three different inputs as described in Fig. 4: (1) signal components with positive polarity (black dotted line); (2) signal components with both positive and negative polarities (red dotted line); and (3) absolute value of the vibro-acoustic signal (blue line).

Fig. 6 shows the results of Savitzky-Golay filtering on the vibro-acoustic signal obtained from a full cycle OLTC operation (i.e. changing one tap position). As shown in this figure, though the filter using the spline curve of peaks in positive polarity can achieve an approximation of the vibro-acoustic signal around its peaks, some components of it slip into the negative side (highlighted in black circles). This is unfavorable for a filter,

This is the author's version of an article that has been published in this journal. Changes were made to this version by the publisher prior to publication.
The final version of record is available at http://dx.doi.org/10.1109/TPWRD.2017.2749374

which is aimed at achieving consistency in extracting vibro-acoustic signal.

As shown in Fig. 5, the Savitzky-Golay filter using the absolute value of the original vibro-acoustic signal exhibits a smoothed approximation of the measured vibro-acoustic signal without compromising its consistency. Also, this filter doesn't exhibit any signal components leakage problem as mentioned in Fig. 5. Therefore, in this study, the absolute value of vibro-acoustic signal, rather than spline curve of its peaks, is fed into the Savitzky-Golay filter as inputs.

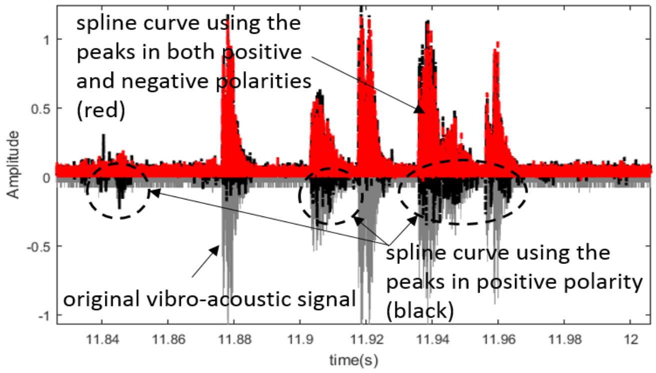

Fig. 6. Results of Savitzky-Golay filtering on the vibro-acoustic signal obtained from a full cycle OLTC operation (i.e. changing one tap position) using (1) spline curve of peaks in positive polarity (in dark black color); and (2) spline curve of peaks in both positive and negative polarities (in red color). The signal components highlighted in the black circles are denoted as those leaked to the negative magnitude.

B. *Savitzky-Golay Filter Parameter Selections*

Selecting the Degree of Polynomial (*N*)

It can be seen from Equations (1) and (2) that with the increase of degree of polynomial, the polynomial curve fits the original signal better and the mean-squared approximation error becomes smaller. However, adopting an excessive polynomial degree may lead to no solution in the signal waveform smoothing and simplification.

Fig. 7 compares the results of five Savitzky-Golay filters, which have the same data size of a frame ($M = 150$) but different orders of polynomial (from the first to the ninth order). It can be seen that the resultant curve of using the Savitzky-Golay filter with the first order polynomial is over-smoothed (i.e. too simplified). It fails to capture the necessary profile of the original signal. On the contrary, the filters with the seventh and the ninth order polynomial lead to a better fitted curve, which tracks the changing trend of the original vibro-acoustic signal. The Savitzky-Golay filter with the fifth order of polynomial shows a balanced performance of simplifying and tracking the changes of the original vibro-acoustic signal.

The frequency spectrums of the outputs of the above filters are plotted in Fig. 8. As the polynomial order decreases, signal components at high frequencies diminish accordingly. Compared to the output of the fifth order filter, the outputs of the first and the third order filters are significantly compromised at 2.5 kHz, which is the frequency corresponding to the mechanical operation of interest from an observational point of view.

Considering a trade-off between the traceability and the simplification of the signal's waveform, the fifth order Savitzky-Golay filter is adopted in this paper for processing OLTC vibro-acoustic signal.

It is worth mentioning that, regardless of the order (N) of polynomial, the output of a Savitzky-Golay filter does not cause a time shift with respect to the original signal. This is a significant advantage when the filter is used for processing multiple types of signals (e.g. vibro-acoustic and arcing signals in the joint OLTC measurement system).

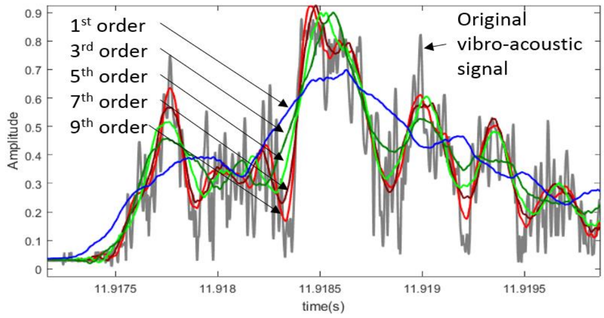

Fig. 7. Results of Savitzky-Golay filters with different orders of polynomial (N = 1, 3, 5, 7, 9) but the same data seize of frame ($M = 150$).

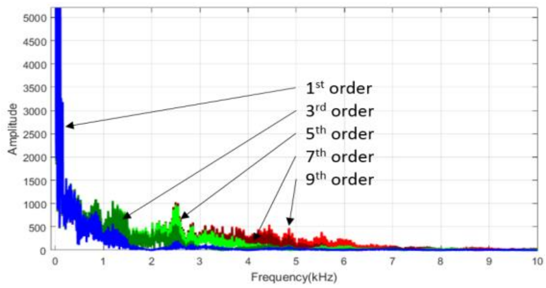

Fig. 8. Frequency spectrum of the outputs of Savitzky-Golay filters with different orders of polynomial from the firth to the ninth order (N = 1, 3, 5, 7, 9) but the same data frame size ($M = 150$).

Selecting the Data Size of a Frame $(2M + 1)$

Along with the degree of polynomial, the data size of a frame $(2M + 1)$ also affects the performance of a Savitzky-Golay filter. Fig. 9 shows the result of five Savitzky-Golay filters with different data frame sizes (M = 50, 200, 350, 500, 650) but the same order of polynomial (the fifth order). Fig. 10 presents the frequency spectrum of the outputs of these filters.

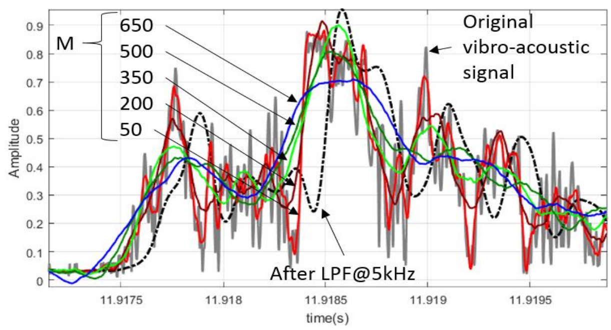

Fig. 9. Outputs of Savitzky-Golay filters with different frame sizes (M = 50, 200, 350, 500, 650) but the same order of polynomial (N = 5).

It can be seen from Fig. 9 that the variation of the data frame sizes of a Savitzky-Golay filter changes the smoothness of the filter's output. With the increase of the data size of a frame (keeping the same polynomial order), the filter can produce more smoothed (simplified) curve over the original signal. This is because more data samples for a data frame of a polynomial results in smoother outputs under the same order (*N*) of a polynomial. This is similar to a situation when a LPF reduces its lower cut-off frequency.

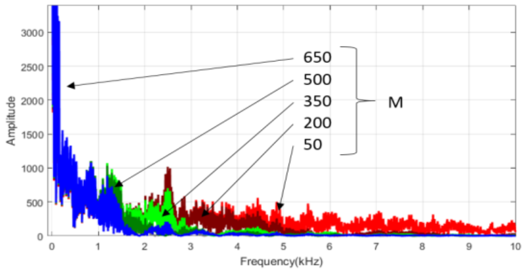

Fig. 10. Frequency spectrum of the outputs of Savitzky-Golay filters with different data frame sizes (M = 50, 200, 350, 500, 650) but the same order of polynomial (N = 5).

As shown in Fig. 9, the Savitzky-Golay filter with the frame size of 1301 (M = 650, blue line) achieves the most smoothed result. However, it cannot properly track the changes in the original signal (i.e. over-smoothed). Moreover, as shown in Fig. 10, its frequency component at 2.5 kHz is significantly reduced compared to the other filters. From Figs. 9 and 10, it can be observed that the filter with a data frame size of 701 (M = 350) presented a good smoothing performance as well as an appropriate traceability of the changes in the original vibro-acoustic signal. The frequency component of this filter at 2.5 kHz is also retained. As a result, the fifth order polynomial and the frame size of 701 (M = 350) is chosen for Savitzky-Golay filtering on OLTC vibro-acoustic signal in this paper.

C. Comparing Savitzky-Golay Filter with Low-Pass Filter and Wavelet's Approximation

As illustrated in Fig. 7 and Fig. 9, the output of a Savitzky-Golay filter always maintains time alignment with the original signal regardless of the output's smoothness. On the contrary, the outputs of wavelet's approximation and LPF cannot maintain time alignment with the original signal. The time delay in the output of a LPF depends on the output's smoothness compared to the original signal by its cut-off frequency. The time shift in the output of a wavelet's approximation is mainly determined by the types of mother wavelet, the number of decomposition level, and the approximation level, of which the signals are reconstructed [11].

Fig. 11 presents the results of applying a Savitzky-Golay filter (N = 5 and M = 350), a wavelet's approximation algorithm, and two LPFs (cut-off frequencies of 3 kHz and 5 kHz) to smooth a vibro-acoustic signal. The vibro-acoustic signal is acquired from an in-service OLTC at the sampling rate of 1 MHz. It can be seen that the Savitzky-Golay filter preserves the profile of the original signal without any time gap.

On the contrary, two LPFs produce time delays of 0.13 and 0.27 millisecond with respect to the original signal respectively. The time delay between the outputs of a LPF and the original signal varies according to the LPF's cut-off frequency. Thus, when there is a change in the cut-off frequency, the time delay will also be changed. This can pose difficulties in analyzing different signals. The factors such as the resonant frequency of OLTC's construction, the sensor type and the configurations of measurement system, and environmental conditions can affect the frequency spectrum of a vibro-acoustic signal. These factors may require a frequent adjustment of a LPF's cut-off frequency, which in turn causes a change in the time delay between the LPF output and the original measured signal.

It can also be observed in Fig. 11, at the time of 1.8003 and 1.8021 second, large gaps exist between the output curve of the wavelet's approximation and the original signal. In these time instances, wavelet's approximation (black cross marked line) has few data points, which results in a time shift to the left side (highlighted in a blue box in the figure). As such, the wavelet's approximation fails to track the changes in the original OLTC vibro-acoustic signal.

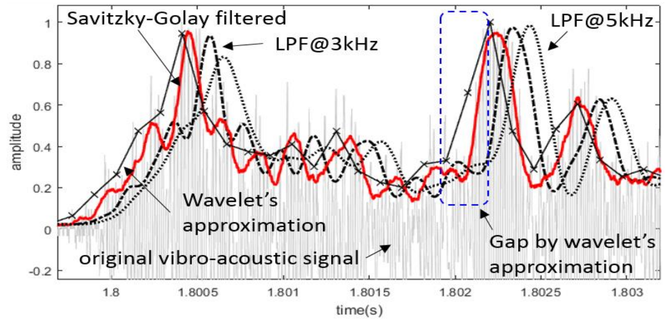

Fig. 11. Comparison of the time shifts in outputs of Savitzky-Golay filter, wavelet's approximation, and low-pass filter.

For the joint vibro-acoustic and arcing signal measurement-based OLTC condition assessment, the time difference caused by wavelet's approximation and LPF can be a critical issue. This is because the vibro-acoustic signal extracted by them cannot be aligned properly with the signals obtained from arcing measurement. Such misalignment can negatively impact the identification of the event sequence during an OLTC operation. This can in turn lead to an inaccurate assessment of its condition.

V. Savitzky-Golay Filter to Analyze Arcing Signal

In Section IV, Savitzky-Golay filtering was applied to analyze vibro-acoustic signal. This section investigates the applicability of Savitzky-Golay filter to extract arcing signal from noise.

In a joint vibro-acoustic and arcing signal measurement system, the arcing signal is acquired by measuring the electromagnetic signal flowing through the transformer's grounding cable or phase connection cables using HFCTs (Fig. 1). In addition to the arcing signal generated by the closing event during OLTC operation, other signals which are the mixture of load current, harmonic, and various interferences and noise may also be picked up by HFCT. This is evidenced in Fig. 12, which shows the field measured arcing signals of two types of OLTCs (i.e. bolt on and column type) [12, 13].

As discussed earlier in this paper, by tuning the parameters (N and M) of a Savitzky-Golay filter, the smoothness of its output waveform can be controlled without causing any time delay. This property can also be utilized to keep high frequency

This is the author's version of an article that has been published in this journal. Changes were made to this version by the publisher prior to publication.
The final version of record is available at http://dx.doi.org/10.1109/TPWRD.2017.2749374

components in the measured arcing signals corresponding to OLTC's switch closing operation and to remove the low frequency components corresponding to load current, harmonics, and noise.

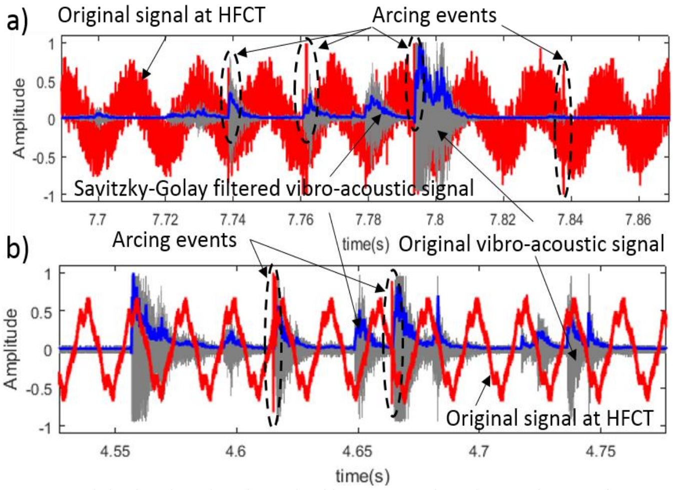

Fig. 12. Original arcing signal acquired by HFCTs clamping on the transformer's grounding cable of (a) bolt on type OLTC; and (b) column type OLTC.

Accordingly, two Savitzky-Golay filters have been designed. One filter is designed for acquiring only high frequency components while the other is designed specifically for the low frequency components. The first filter has the parameters of a ninth order polynomial and data frame size of 101 (M = 50) while the second filter has a polynomial order of zero and data frame size of 1301 (M = 650). The results of the two filters are drawn in Fig. 13. In this figure, the signal plotted in black color is the output of the first Savitzky-Golay filter (the filter keeps high frequency components) and the signal plotted in green color is the output of the second filter (the filter keeps low frequency components). Since the Savitzky-Golay filter doesn't cause any time gap regardless of parameters, the outputs of both filters in Fig. 13 are well synchronized.

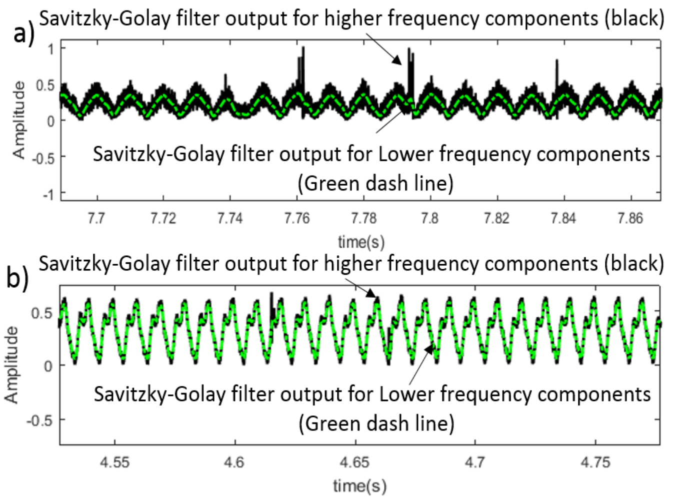

Fig. 13. Results of two Savitzky-Golay filters (black signal is the output of the filter for keeping high frequency components; green signal is the output of the filter for keeping low frequency components) of (a) bolt on type OLTC; and (b) column type OLTC.

The lower frequency components (related to load current, harmonics, and noise) embedded in the measured arcing signal can be removed by subtracting the output of the second filter from that of the first filter. Subtraction eliminates low frequency components while preserving high frequency components (as shown in Fig. 14).

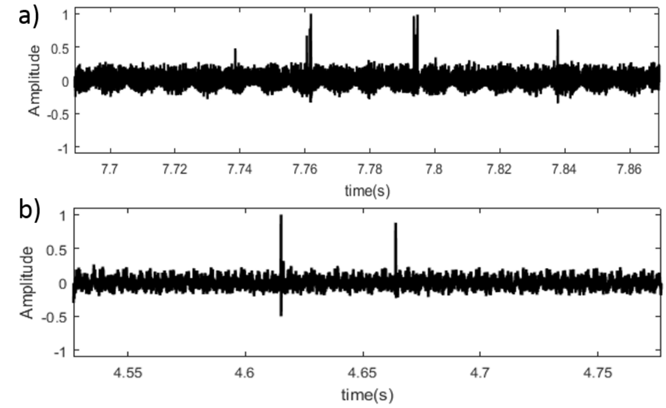

Fig. 14. Extracted arcing signals (a) bolt on type OLTC; and (b) column type OLTC.

Finally, a threshold is applied to the remaining high frequency components in Fig. 14 to extract pure arcing signal caused by a switch's closing event during OLTC operation. The results are shown in Fig. 15.

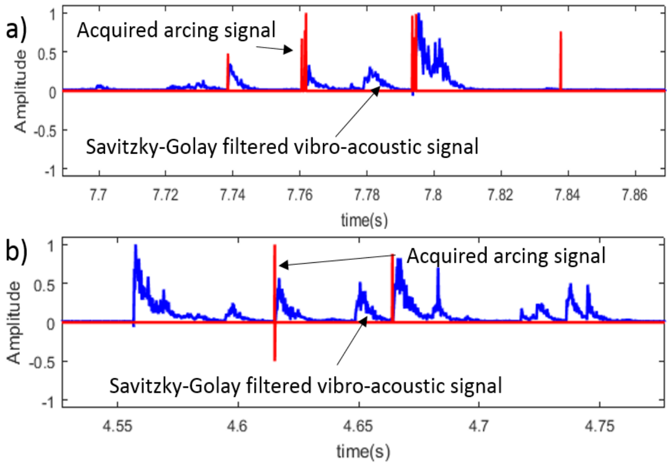

Fig. 15. Processed and filtered vibro-acoustic signal (blue) and arcing signal (red) by Savitzky-Golay filter (a) bolt on type OLTC; and (b) column type OLTC.

It is worth mentioning that in field environment, arcing signal may also be corrupted by other types of complex noise signals. These noise signals can be removed by using other digital signal processing techniques, for example, the probabilistic wavelet transform [14]. However, as shown above, Savitzky-Golay filter can separate arcing signal from noise, power frequency and harmonics successfully.

VI. Application of Savitzky-Golay Filter to Extract Phase Information from Arcing Signal

In the previous discussions on arcing signal extraction, it is implicitly assumed that the arcing signals flowing into transformer's phase connection cable or grounding cable are solely caused by the switch's closing event in OLTC's operation. However, in reality, other types of discharges caused by the insulation defects inside a transformer can also flow into transformer's grounding/phase connection cables. These

This is the author's version of an article that has been published in this journal. Changes were made to this version by the publisher prior to publication.
The final version of record is available at http://dx.doi.org/10.1109/TPWRD.2017.2749374

discharge signals can be extracted with the arcing signal. It is therefore necessary to distinguish arcing signals generated by OLTC's operation from other types of discharges generated by transformer insulation defects.

The different types of electrical discharge can be identified using the phase location of the discharge impulses. Thus the phase angle of the transformer AC voltage needs to be recorded [15, 16]. The phase angle can be directly measured from AC voltage which requires a separate data acquisition channel on the hardware. For a three-phase OLTC joint vibration and arcing measurement system, it requires at least one vibro-acoustic signal measurement and three HFCT measurements on each phase. This section investigates the possibility of applying Savitzky-Golay filter to extract phase information from the signals measured by the HFCTs.

Fig. 16a shows the AC voltage signal measured from a wall socket in the substation, in which the online condition monitoring of OLTCs were conducted. Fig. 16b and Fig. 16c show the signals measured from HFCTs clamped on a phase cable and a grounding cable respectively.

It can be seen from Fig. 16b, the measured signal (acquired from phase connection cable) is a mixture of load current, harmonics, and arcing signal generated during OLTC operation. The dominant energy in frequency spectrum occurs at 50 Hz followed by harmonics at 250 Hz and 350 Hz (right side graph in Fig.16b). Since the 50 Hz load current signal is distorted, it is difficult to extract phase information from this signal directly. However, as shown below, Savitzky-Golay filter can extract phase information from the mixture of signals in Fig. 16b.

It can be seen from Fig. 16c (right side graph) the measured signal (acquired from the grounding cable) is dominated by DC and 50 Hz, and is followed by harmonics at 250 Hz and 350 Hz. It looks impossible to extract phase information from this signal. However, even in this case, Savitzky-Golay filter can extract phase information from this signal.

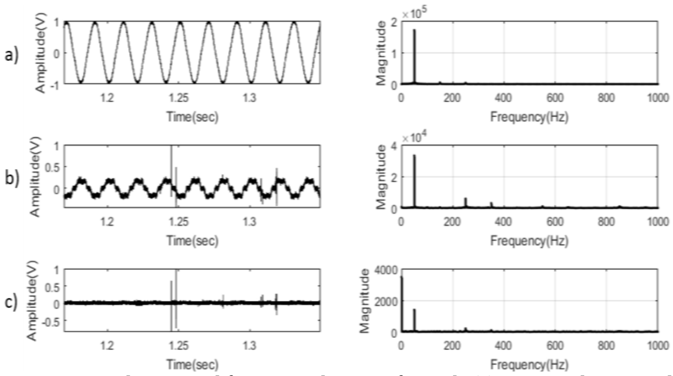

Fig. 16. Time domain and frequency domain of signals (a) AC signal measured from a wall socket of the transformer under investigation; (b) current signal measured by a HFCT clamped on a phase connection cable; and (c) current signal measured by a HFCT clamped on the grounding cable.

For retrieving AC phase information from the current signals in Fig. 16b and Fig. 16c using Savitzky-Golay filter, signal components at lower frequency (around AC power frequency) should be taken and signal components at higher frequency should be minimized. As such, the zero order polynomial and frame size of M = 650 are used for this application. After Savitzky-Golay filtering, DC offset can be removed by subtracting the mean value of the current signal. Finally, only the signal around AC power frequency is extracted without causing any time delay while removing harmonics, noise, and arcing signal. This signal can be synchronized with the extracted vibro-acoustic and arcing signals.

Fig. 17a shows the extracted AC waveform by Savitzky-Golay filtering on the signal measured at a phase connection cable. It can be seen that this AC waveform becomes clearer and the phase information can be extracted as shown in Fig. 17b. More interestingly, Savitzky-Golay filter can extract AC waveform from the signal measured at the grounding cable (Fig 17c and Fig. 17d) though the signal is dominated by DC component (Fig. 16c).

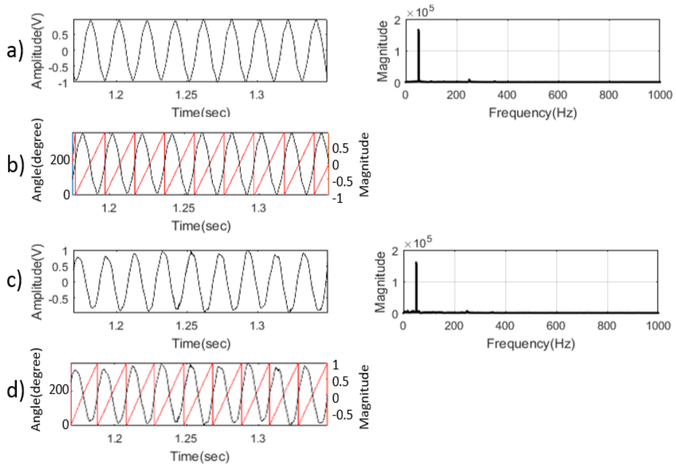

Fig. 17. (a) Extracted AC cycle and its frequency spectrum from the signal measured at a phase connection cable; (b) phase information obtained from Fig. 17a; (c) extracted AC cycle and its frequency spectrum from the signal measured at a grounding cable; (d) phase information obtained from Fig. 17c.

VII. Case Studies of Savitzky-Golay Filtering on the Joint Vibration and Arcing Measurement of OLTC

Throughout Section IV to Section VI, a number of important applications of Savitzky-Golay filter for OLTC condition monitoring were presented. This section demonstrates that an integration of these applications (vibro-acoustic signal extraction, arcing signal extraction, and phase information recovery from arcing signal) can improve the interpretability of the signals obtained from the joint measurement system for OLTC condition monitoring.

Fig. 18 and Fig. 19 present the results of applying Savitzky-Golay filter to process the vibro-acoustic and arcing signals measured from two different types of OLTCs (bolt-on type in Fig. 18 and column type in Fig. 19) and subsequently correlate the vibro-acoustic and arcing signals with the operational sequences of the two OLTCs during changes to the tap positions.

Fig. 18a and Fig. 19a show the originally acquired vibro-acoustic (blue) and arcing signals (red) of the two OLTCs. It can be seen that the vibro-acoustic signals consist of a series of bursts, of which the event time is ambiguous. Also, the arcing signals are heavily embedded in the harmonics and noise. Without processing the originally measured signals, it would be difficult to correlate these signals to the corresponding OLTC's

The final version of record is available at http://dx.doi.org/10.1109/TPWRD.2017.2749374

operational sequence. Fig. 18b and Fig.19b depict the OLTC's operational timing diagrams of bolt-on type and column type respectively. The results of Savitzky-Golay filtering on the originally measured vibro-acoustic and arcing signals of these two OLTCs are plotted in Fig. 18c and Fig.19c, respectively.

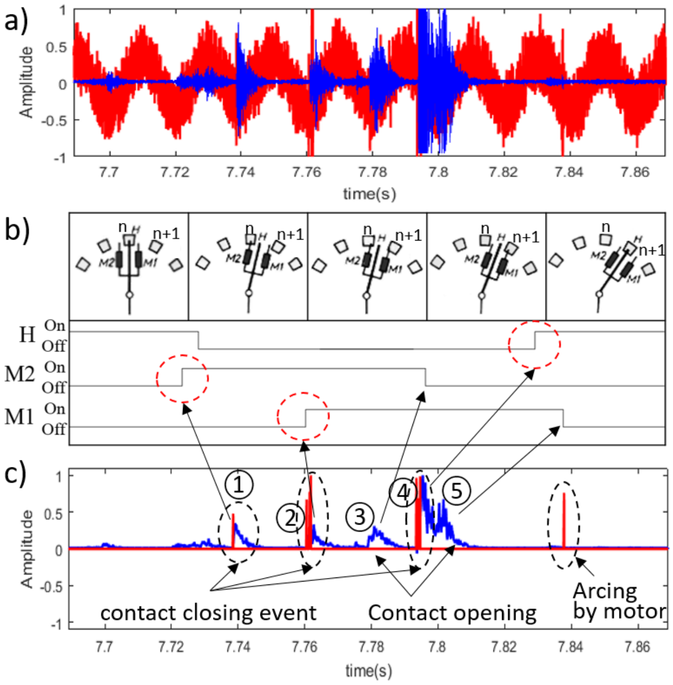

Fig. 18. (a) Originally measured vibro-acoustic signal (in blue) and arcing signal (in red) from a bolt-on type OLTC when it moves from the tap position n to the tap position $n + 1$; (b) timing diagram of the OLTC's contacts; and (c) results of Savitzky-Golay filtering on vibro-acoustic and arcing signals (red impulses are the arcing signals extracted and blue signals are the vibro-acoustic signals smoothed by Savitzky-Golay filters). H – main contact, M1 – transition contact, M2 – transition contact.

For the bolt-on type OLTC, all arcing signals are generated when a main or two transition switches are in closing event. The signals corresponding to the three switches' closing events are successfully extracted by Savitzky-Golay filter and can be clearly identified in Fig. 18c (red color impulses). The last arcing event shown in Fig. 18c is caused by motor stop operation, which is also confirmed by the CT measurement on the OLTC's motor [6]. With reference to the extracted arcing signals, the smoothed vibro-acoustic signals in Fig. 18c can be properly interpreted. Each individual vibro-acoustic signal (in blue color) corresponding to a particular step in OLTC's operation is described as follows:

(1) The OLTC starts to change its tap position at tap position *'n'*, the transition contact 'M2' closes at tap position *'n'* generating vibro-acoustic signal '1' and shortly after that , the main contact 'H' opens at tap position *'n'*;
(2) The transition contact 'M1' closes at tap position *'n+1'* generating vibro-acoustic signal '2';
(3) The transition contact 'M2' opens at tap position *'n'* generating vibro-acoustic signal '3';
(4) The main contact 'H' closes at tap position *'n+1'* generating vibro-acoustic signal '4';
(5) The transition contact 'M1' opens at tap position *'n+1'* generating vibro-acoustic signal '5'. The OLTC completes changing its tap position from *'n'* to *'n+1'*.

In case of column type OLTC, closing events of vacuum switches in main and transition generated arcing signals. The arcing signals corresponding to the two contact switches' closing events are successfully extracted by the Savitzky-Golay filter and can be clearly identified in Fig. 19c (red color signal). Also, as shown in Fig. 19c, the vibro-acoustic signals (blue color signals) are simplified by the Savitzky-Golay filter. With reference to the extracted arcing signals, the smoothed vibro-acoustic signals in Fig. 19c can be properly interpreted. Each individual vibro-acoustic signal (in blue color) corresponding to a particular step in OLTC's operation is described as follows:

(1) The OLTC starts to change its tap position at tap position '*n*', the transition switch (TTS) opens at tap position '*n*' generating vibro-acoustic signal '1';
(2) The transition vacuum switch (TTV) opens at tap position '*n*' generating vibro-acoustic signal '2';
(3) The transition switch (TTS) closes at tap position '*n*+1' generating vibro-acoustic signal '3';
(4) The transition vacuum switch (TTV) closes at tap position '*n*+1' generating vibro-acoustic signal '4';
(5) The main vacuum switch (MSV) opens at tap position '*n*' generating vibro-acoustic signal '5';
(6) The main switch (MTS) opens at tap position '*n*' generating vibro-acoustic signal '6';
(7) The main switch (MTS) closes at tap position '*n*+1' generating vibro-acoustic signal '7';
(8) The main vacuum switch (MSV) closes at tap position '*n*+1' generating vibro-acoustic signal '8'. The OLTC completes changing its tap position from '*n*' to '*n*+1'.

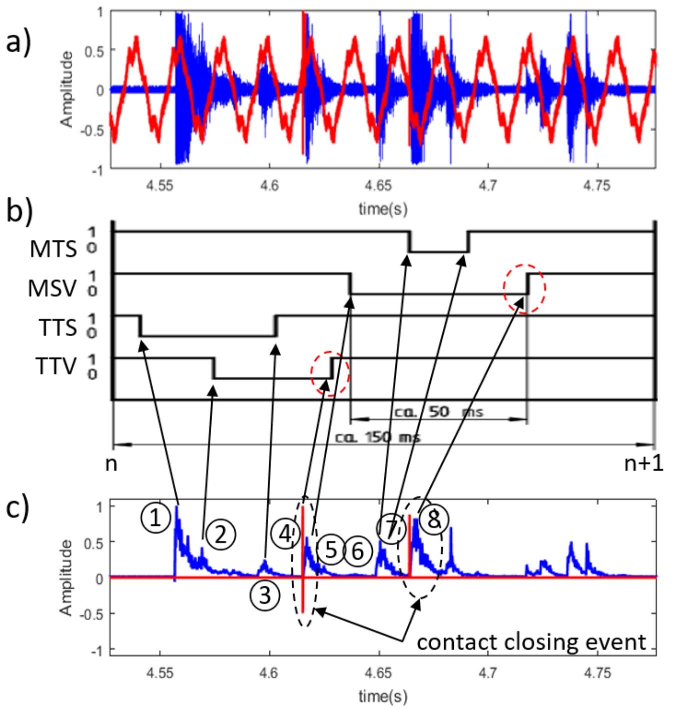

Fig. 19. (a) Originally measured vibro-acoustic signal (in blue) and arcing signal (in red) acquired from a column type OLTC when it moves from the tap position n to the tap position $n + 1$; (b) timing diagram of OLTC contacts; and (c) results of Savitzky-Golay filters for processing vibro-acoustic and arcing signals (red impulses are the arcing signals extracted and blue signals are the vibro-acoustic signals smoothed by Savitzky-Golay filters). MTS – main switch, MSV – main vacuum switch, TTS – transition switch, TTV – transition vacuum switch.

As it can be seen from Fig. 18 and Fig. 19, the filtered vibro-acoustic signal and the extracted arcing signal by the Savitzky-Golay filter are synchronized without any time gap compared with the original vibro-acoustic signal and arcing signal.

Furthermore, Fig. 20 shows the results of applying the Savitzky-Golay filter to extract phase information on the above two types of OLTC.

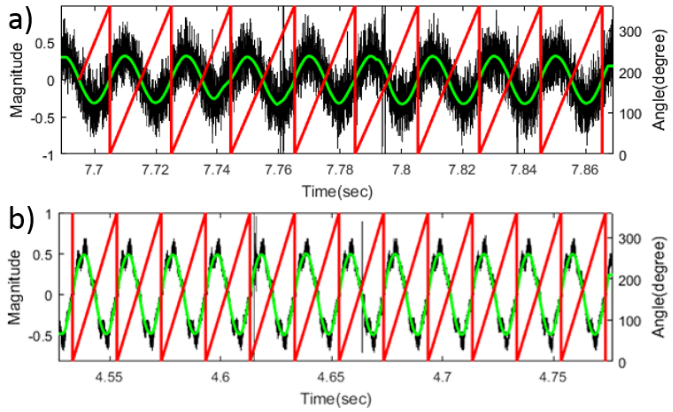

Fig. 20. Results of phase information from a current signal at a phase connection cable (a) bolt-on type OLTC; and (b) column type OLTC (signal in black color – original current signal; signal in green color – processed signal; signal in red color – phase information from the processed signal).

The above case studies proved that the Savitzky-Golay filters can attain reliable performance of smoothing and filtration for the signals acquired by the joint vibration and arcing measurement system for OLTC condition monitoring. It was achieved with the unique benefits of Savitzky-Golay filters; not causing a time gap regardless of the level of filtration.

After a relatively long period of service, an OLTC may experience different kinds of mechanical problems such as coking on switches and contacts, misalignments on contacts, spring looseness, motor drive system's defects, and defects in gears and cams, etc. [3]. The ultimate aim of OLTC condition monitoring is to recognize different types of mechanical problems, which can impair the normal operation of OLTC and even cause the failure of the whole transformer.

The joint vibro-acoustic and arcing measurement system and Savitzky-Golay filtering can provide the visibility of the operation of OLTC. On the other hand, any mechanical condition changes in OLTC's switches and contacts, springs, motor drive system, gears and cams can reflect on the measured vibro-acoustic and arcing signals. Thus, there may exist some correlations between the types of OLTC's mechanical problems and the characteristics of vibro-acoustic and arcing signals extracted by Savitzky-Golay filters. The authors are further investigating on how the different kinds of OLTC defects affect vibro-acoustic signals and how the different condition of contacts affects the amplitudes of arcing signals. It is expected that a database can be established consisting of different types of OLTC mechanical problems and the corresponding vibro-acoustic and arcing signals extracted by the Savitzky-Golay filter. With such a built-in database, the joint vibro-acoustic and arcing measurement system can provide condition assessment and fault identification of OLTC.

VIII. Conclusions

This paper successfully applied the Savitzky-Golay filter to analyze signals from the joint vibration and arcing measurement system installed on OLTCs. It has been demonstrated that, with the merits of easy implementation and no distortions in its outputs, the Savitzky-Golay filter can achieve:

a) Envelope curve extraction from vibro-acoustic signal.
b) Arcing signal extraction.
c) Phase information extraction from arcing signal.

The future work will be the use of the above information for establishing fingerprints with respect to different mechanical conditions of OLTC.

Acknowledgment

The authors gratefully acknowledge Australian Research Council and industry partners AusGrid, Ergon Energy, Powerlink Queensland, TransGrid and Wilson Transformer Company Pty Ltd, for providing supports for this work. Thanks are due to Energex for providing access to OLTC measurements.

References

[1] P. Kang and D. Birtwhistle, "Condition assessment of power transformer on-load tap-changers using wavelet analysis," IEEE Transactions on Power Delivery, vol. 16, pp. 394-400, 2001.

[2] P. Kang and D. Birtwhistle, "Condition monitoring of power transformer on-load tap-changers. Part 1: Automatic condition diagnostics," IEEE Proceedings: Generation, Transmission and Distribution, vol. 148, pp. 301-306, 2001.

[3] T. Bengtsson, H. Kols, L. Martinsson, B. O. Stenestam, M. Foata, F. Leonard, C. Rajotte, and J. Aubin, "Acoustic diagnosis of tap changers," CIGRE SC 12, 1996.

[4] E. Rivas, J. C. Burgos, and J. C. Garcia-Prada, "Condition assessment of power OLTC by vibration analysis using wavelet transform," IEEE Transac tions on Power Delivery, vol. 24, pp. 687-694, 2009.

[5] E. Rivas, J. C. Burgos, and J. C. Garcia-Prada, "Vibration analysis using envelope wavelet for detecting faults in the OLTC tap selector," IEEE Transactions on Power Delivery, vol. 25, pp. 1629-1636, 2010.

[6] J. Seo, H. Ma and T.K. Saha, "A Joint Vibration and Arcing Measurement System for Online Condition Monitoring of On-Load Tap Changer of Power Transformer," IEEE Transactions on Power Delivery, vol. 32, pp. 1031-1038, 2017.

[7] A. Krämer, J. MEYER, J. A. J. PETTINGA, R. JANUS, and V. SEITZ, " Monitoring Methods for On-load Tap-changers. An Overview and Future Perspectives," CIGRÉ 1996 : 12-108.

[8] A. Savitzky and M. J. E. Golay, "Smoothing and Differentiation of Data by Simplified Least Squares Procedures," Analytical Chemistry, vol. 36, pp. 1627-1639, 1964.

[9] R. Schafer, "What is a savitzky-golay filter?" IEEE Signal Processing Magazine, vol. 28, pp. 111-117, 2011.

[10] R. Schafer, "On the frequency-domain properties of Savitzky-Golay filters, "Digital Signal Processing Workshop and IEEE Signal Processing Education Workshop, 2011.

[11] S. Qian, "Introduction to Time-Frequency and Wavelet Transforms," Prentice Hall PTR, ISBN-10: 0130303607, 2002.

[12] ABB, "On-load tap-changers, type UZ Technical guide," 2003.

[13] REINHAUSEN, "REINHAUSEN OLTC VACUTAP VV Operating Instructions," 164/08 EN.

[14] J. Seo, H. Ma, and T. K. Saha, "Probabilistic wavelet transform for partial discharge measurement of power transformer," IEEE Transactions on Dielectrics and Electrical Insulation, vol. 22, no. 2, pp. 1105-1117, 2015.

[15] F. H. Kreuger, "Partial Discharge Detection in HV Equipment," London Butterworth, UK, 1989.

[16] IEC 60270-2000, "High Voltage Test Techniques - Partial Discharge Measurements".

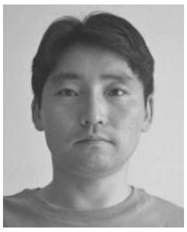

Junhyuck Seo (S'13) received the B.Eng. degree in Electrical Engineering from Gyeongsang National University, Jinjiu, South Korea, in 2001 and the M.Phil. degree in Electrical Engineering from the University of Queensland, Brisbane, Australia, in 2014, where he is currently pursuing the Ph.D. degree in information technology and electrical engineering. He was an Engineer and Senior Engineer with Hyundai Motor, South Korea, from 2000 to 2012. His research interests include signal processing for condition assessment of power transformers.

Hui Ma (M'95-SM'16) received the B.Eng. and M.Eng. degrees in Electrical Engineering from Xi'an Jiaotong University, Xi'an, China, in 1991 and 1994, respectively, the M.Eng. (by research) degree in Electrical Engineering from Nanyang Technological University, Singapore in 1998, and the Ph.D. degree in Electrical Engineering from the University of Adelaide, Adelaide, Australia, in 2008. Currently, he is a Research Fellow with the School of Information Technology and Electrical Engineering, the University of Queensland, Brisbane, Australia. Prior to joining the University of Queensland, he spent many years on research and development. From 1994 to 1995, he was a Researcher with Xi'an Jiaotong University. From 1997 to 1999, he was a Firmware Development Engineer with CET Technologies Pte. Ltd., Singapore. He was a Research Engineer with Singapore Institute of Manufacturing Technology from 1999 to 2003. His research interests include industrial informatics, condition monitoring and diagnosis, power systems, wireless-sensor networks, and sensor signal processing.

Tapan Kumar Saha (M'93-SM'97) was born in Bangladesh in 1959 and immigrated to Australia in 1989. He received the B.Sc. degree in engineering (electrical and electronic) from the Bangladesh University of Engineering & Technology, Dhaka, Bangladesh, in 1982, the M.Tech. degree in electrical engineering from the Indian Institute of Technology, New Delhi, India, in 1985, and the Ph.D. degree in Electrical Engineering from the University of Queensland, Brisbane, Australia, in 1994. Currently, he is Professor of Electrical Engineering with the School of Information Technology and Electrical Engineering, University of Queensland. Previously, he had visiting appointments for a semester at both the Royal Institute of Technology (KTH), Stockholm, Sweden and at the University of Newcastle, Newcastle, Australia. His research interests include condition monitoring of electrical plants, power systems, and power quality. Prof. Saha is a Fellow of the Institution of Engineers, Australia.